

Effect of coagulation conditions on size and morphology of phytoplanktonic organism aggregates

Wpływ warunków koagulacji na wielkość i morfologię agregatów organizmów fitoplanktonowych

Ph.D. Ewelina Kapuścińska ^{*)}

Keywords: *coagulation, particle morphology, fractal geometry, image analysis.*

Abstract

This paper presents results of research on changes in morphological parameters and fractal dimensions of *Monoraphidium contortum* and *Microcystis aeruginosa* cell aggregates obtained from coagulation using FeCl_3 . The study used Morphologi G3 as microscopic image analyzer. Based on the microscopic image analysis, the aggregates specific morphological parameters were determined: equivalent diameter (d_e), „elongation”, „solidity” and aggregate fractal dimensions – D_1 and D_2 . It was found that, size of phytoplankton cell aggregates was subordinated to log-normal distribution. The analysis of changes in aggregate size distribution indicated that along with the increase of coagulant doses (D_c) and flocculation time (t_f), their mean equivalent diameter increased. The average diameter of aggregates, on the other hand, decreased with increasing velocity gradient (G). Along with the increase in the amount of energy introduced into the system during mixing (G), a tendency to elongate cell aggregates and reduce their solidity was observed. The morphological characteristics of phytoplankton aggregates based on morphological parameters and fractal geometry allowed to observe a significant relationship between D_2 and „solidity”. An increase in the morphological parameter in the form of „solidity” was associated with an increase in the value of the second fractal dimension. Aggregate size evolution, at a constant velocity gradient, occurred in three stages: aggregate growth (I), aggregate break-up (II) and steady state (III). The size and spatial structure of aggregates influenced sedimentation properties of flocs. The reduction of the mean equivalent diameter and solidity of aggregates resulted in a slower sedimentation rate of aggregates.

Słowa kluczowe: *koagulacja/flokulacja, morfologia cząstek, geometria fraktalna, analiza obrazu.*

Streszczenie

W pracy poddano analizie zmiany parametrów morfologicznych i wymiarów fraktalnych agregatów komórek zielenicy *Monoraphidium contortum* oraz sinicy *Microcystis aeruginosa* „uzyskanych w wyniku koagulacji prowadzonej z wykorzystaniem chlorku żelaza (III). W badaniach wykorzystano analizator obrazu Morphologi G3. Zastosowana metoda cyfrowej analizy obrazu mikroskopowego pozwoliła na scharakteryzowanie zarejestrowanych cząstek za pomocą szeregu parametrów morfologicznych: średnica równoważna (d_e), „wydłużenie”, „zwarłość”. Ponadto, w oparciu o analizę obrazu mikroskopowego, wyznaczono wymiary fraktalne – D_1 i D_2 . Stwierdzono, że wielkość agregatów komórek fitoplanktonu była podporządkowana rozkładowi log-normalnemu. Przeprowadzona analiza zmian rozkładów wielkości agregatów wskazała, że wraz ze wzrostem dawek koagulantu (D_k) i czasu flokulacji (t_f) następował wzrost ich średniej średnicy równoważnej. Średnia średnica agregatów uległa natomiast zmniejszeniu wraz ze wzrostem gradientu prędkości (G). Zwiększanie ilości energii wprowadzanej do układu podczas mieszania (G), prowadziło do wydłużania się agregatów komórek oraz zmniejszania ich zwarłości. Charakterystyka morfologiczna agregatów fitoplanktonu, oparta na parametrach morfologicznych i geometrii fraktalnej pozwoliła zaobserwować istotną zależność pomiędzy D_2 , a „zwarłością”. Wzrost parametru morfologicznego w postaci „zwarłości” związany był ze zwiększeniem wartości drugiego wymiaru fraktalnego. Zaobserwowano, że zmiana wielkości agregatów w czasie, przy stałym gradientcie prędkości zachodziła w trzech etapach: wzrost agregatów (I), rozpad agregatów (II) i ustalenie stanu równowagi (III). Wielkość i struktura przestrzenna agregatów wpływała na właściwości sedymentacyjne kłaczków. Zmniejszenie średniej średnicy równoważnej i zwarłości agregatów decydowało o mniejszej prędkości sedymentacji agregatów.

1. INTRODUCTION

Water supply systems, whose source of supply are surface waters, are struggling with the problem of „water bloom” during summer. The massive growth of phytoplankton organisms in water reservoirs intended for water intake for the purposes of supplying the population with drinking water, results in its quality parameters deterioration. Depending on the abundance and

species composition of phytoplankton, changes in organoleptic, bacteriological and physicochemical properties of water are observed, causing it to become unusable for consumption. During treatment of water contaminated with phytoplankton suspension, technological difficulties arise, mainly due to the low efficiency of aggregation and separation of already aggregated material. Penetration of single phytoplankton cells or their aggregates into

^{*)} Ph.D. Ewelina Kapuścińska, <https://orcid.org/0000-0002-1003-8462>, Lodz University of Technology, Faculty of Civil Engineering, Architecture and Environmental Engineering, Institute of Environmental Engineering and Building Installations, Politechniki 6 Street, 90-924 Lodz, Poland, corresponding address: ewelina.gutkowska@p.lodz.pl, Politechnika Łódzka, Wydział Budownictwa, Architektury i Inżynierii Środowiska, Instytut Inżynierii Środowiska i Instalacji Budowlanych, al. Politechniki 6, 90-924 Łódź, adres korespondencyjny: ewelina.gutkowska@p.lodz.pl

the subsequent stages of treatment, storage and distribution of water, generate serious problems associated with the presence of pathogenic microorganisms and toxic substances. Especially dangerous, in the case of water containing phytoplankton, is the use of chlorination disinfection. This produces chloroorganic compounds, among which the group of trihalomethanes (THMs) are dominant, which are classified as potentially carcinogenic factors to humans [25].

Difficulties in the aggregation of phytoplankton result from their numerous adaptations, a diversified degree of morphological organization, high number of organisms and their high dispersion degree [2, 21, 23, 26]. For a long time, in the water treatment processes containing phytoplankton suspension, a coagulation using hydrolysing metal salts has been used. The problem is to determine the appropriate conditions for the process of phytoplankton cell aggregation and selection of an effective method of their separation. The analyzes carried out so far on elimination of phytoplankton cells from water, omitted the issue of aggregate morphology formed in the process of coagulation and flocculation. Knowledge about the spatial structure of particles allows a better understanding of their aggregation and degradation that occur in the flocculating system. It is possible to determine the optimal conditions, in which the coagulation and flocculation process should be carried out, to ensure the highest efficiency of cell aggregation. In addition, depending on the size of the aggregates, their morphological characteristics and resistance to disintegration, different separation processes are used.

Determining the complex structure of aggregates formed in the flocculation process is possible thanks to the image analysis techniques [1, 4]. Microscopic image analysis allows to characterize the diverse, irregular shape of aggregates using a number of morphological parameters (e.g. „solidity”, „elongation”) and fractal dimensions (D_1 and D_2) [17, 19, 20].

The aim of the study was to determine the effect of coagulant dose (D_c), velocity gradient (G) and slow mixing time (t_f) on the size and shape of the aggregates of *Monoraphidium contortum* and *Microcystis aeruginosa* cells. The effect of morphological parameters of aggregates on their sedimentation properties was also determined.

2. Materials and method

2.1. Materials

For the study purposes cell suspensions of *Monoraphidium contortum* (Chlorophyta), and *Microcystis aeruginosa* (Cyanobacteria) were used. Both species are commonly found in eutrophic waters, affecting the deterioration of physical, chemical and organoleptic properties of water [5, 10]. *M. contortum* and *M. aeruginosa* are characterized by a different morphological structure, which allowed to verify the effect of cell size and shape on the spatial structure of formed aggregates. Individual *M. contortum* cells have a spindle-like, elongated shape, reaching 16-18 μm in length and 2 μm in width. In contrast, *M. aeruginosa* are spherical shaped cells. The diameter of a single cell is between 2.6 and 5.4 μm . The presence of *M. aeruginosa* cells in drinking water is hazardous to health due to the production of hepatotoxins – microcystins [9, 24]. According to Falconer and Humpage [11], microcystins are promoters of cancer tumors.

M. aeruginosa and *M. contortum* cell suspensions were obtained from the University of Gdansk. Cyanobacteria were proliferated in laboratory conditions in 20 L glass flasks using Z-8 medium [18]. Algae were proliferated in laboratory conditions in 20 L glass flasks using F/2 (algae) medium according to a recipe obtained from the University of Gdansk. The growth of both species of phytoplankton took place at a temperature of 20-25°C,

using artificial lighting (fluorescent lamp OSRAM L18W/11-860 Lumilux Plus Eco – 1300 lm). Photoperiod was 16 hours. Tests and measurements were carried out using a suspension of phytoplankton organisms taken from a flasks, after diluting with distilled water in 1:10 ratio. The use of a higher concentration of phytoplankton suspension prevented the morphological analysis of aggregates using digital microscopic image analysis due to insufficient floc dispersion.

2.2 Coagulation and flocculation procedures

This experiment examined the effect of coagulant dose (D_c), mixing intensity (G) and flocculation time (t_f) on the size and morphological structure of the aggregates formed. Process conditions are presented in the Table 1. The flocculation chambers were polyethylene beakers with active capacity of 1 L, height 130 mm and diameter 100 mm. Because of the greater efficiency of phytoplankton cell aggregation using iron coagulants compared to aluminum coagulants [13, 25], the $\text{FeCl}_3 \cdot 6\text{H}_2\text{O}$ was used. The pH was corrected to a constant pH value 6.0 ± 0.1 using HCl and NaOH solutions. A JLT-6 multi-position mixer from Velp Scientifica (Italy) with 75×25 mm flat paddle impeller was used in the study. Water samples were taken in the final phase of slow mixing and transferred to a *wet cell* plate (100×80 mm). The plate was then placed in a image analyzer (Morphologi G3 from Malvern), using which the particle size and morphological parameters were measured. The tests were carried out at 23.0 ± 0.1 °C.

Table 1. Parameters of the coagulation and flocculation process used during the study

Tabela 1. Parametry procesu koagulacji i flokulacji zastosowane w badaniach

Variable process parameter	Variable values	Constant process parameters		
Coagulant dose, D_c	1-40 mg $\text{Fe}^{+3} \cdot \text{L}^{-1}$	$t_f = 10$ min.	pH = $6.0 \pm 0,1$	$G = 4 \text{ s}^{-1}$
Velocity gradient, G	4, 21, 46, 131, 240 s^{-1}	$D_c = 20$ mg $\text{Fe}^{+3} \cdot \text{L}^{-1}$	pH = $6.0 \pm 0,1$	$t_f = 20$ min.
Flocculation time, t_f	0-60 min.	$D_c = 20$ mg $\text{Fe}^{+3} \cdot \text{L}^{-1}$	pH = $6.0 \pm 0,1$	$G = 4 \text{ s}^{-1}$

In the reaction vessel, the hydrodynamic conditions were characterized by the velocity gradient G calculated according to the relationship [3, 4]:

$$G = \sqrt{\frac{P_m}{\mu \cdot V}} \quad (1)$$

where P_m is power input into the mixing tank ($\text{kg} \cdot \text{m}^2 \cdot \text{s}^{-3}$), V is the stirred tank volume (m^3), μ is dynamic viscosity ($\text{kg} \cdot \text{m}^{-1} \cdot \text{s}^{-1}$). Power inserted into the mixing liquid P_m was determined basing on the relation of the mixer blades number m [-], their width b [m], the density of the liquid ρ [$\text{kg} \cdot \text{m}^{-3}$], hydraulic resistance ratio ζ [-], the rotational speed of the stirrer n_m [s^{-1}] and paddles radius r [m]:

$$P_m = m \cdot \pi^3 \cdot \rho \cdot \zeta \cdot n_m^3 \cdot b \cdot r^4 \quad (2)$$

2.3. Analysis of aggregates properties

The size and morphology of aggregates formed in the reaction vessel were determined by image analysis. Microscopic image analyzer Morphologi G3 is a fully automated system ensuring high quality image and detailed analysis of the size, shape and number of particles. The measuring system of the Morphologi G3 analyzer includes an automatic microscope and a computer with software enabling the measurements and analysis of the results. Morphological parameters were based on the relationship

between the geometric characteristics of the analyzed particles (aggregate) projection area (Table 2). These features included: the area of the particle projection (A), area defined by the thread surrounding a particle (A_t), width (w) and maximum length of the particle (l). The morphological parameters analyzed in this paper met the most important criteria in the morphological characteristics of the particles, they corresponded to the shapes observed based on optical microscopy and their values were normalized in the range of 0-1, which is in accordance with the requirements of norm *Representation of results of particle size analysis. Part 6: Descriptive and quantitative representation of particle shape and morphology* [14].

Table 2. Definitions of the particle morphology parameters

Tabela 2. Parametry morfologiczne cząstek

Morphology parameters	Formula	Comments
Equivalent diameter (d_e)	$d_e = 2 \sqrt{\frac{A}{\pi}}$	Equivalent diameter – the diameter of a circle with the same area, as the image of the analyzed particle.
Solidity (S)	$S = \frac{A}{A_t}$	Solidity – the ratio of the actual particle area to the area of the figure designated by the stretched thread which surrounds the particle. Solidity also has values in the range 0-1 (perfect circle).
Elongation (E)	$E = 1 - \frac{w}{l}$	Elongation – the ratio of width to the length of the analyzed particles. Elongation values in the range from 0 (circular particle) to 1.

The first and second fractal dimensions were determined using aggregates projection surface (A), their perimeter (P) and maximum length (l) (Table 3). Appropriate interpretation of the determined values of fractal dimensions allows to determine the spatial structure of aggregates. According to Oliveira et al. [19] aggregates which D_2 value tends to 0 have an open, highly branched and loose structure, while the value D_2 close to 2 may suggest a more compact structure. A similar interpretation is presented in article Jiang and Logan [16] and Chakraborti et al. [7] indicating that the particle with $D_2 < 2$ have a more porous structure.

Table 3. Definitions of fractal dimensions used in the study

Tabela 3. Wymiary fraktalne wykorzystane w badaniach

Fractal dimension	Formula	Comments
First fractal dimension (D_1)	$P \propto l^{D_1}$	The degree of irregularity of the particles perimeter P
The second fractal dimension (D_2)	$A \propto l^{D_2}$	The degree of increase of the surface area A of the particles to its maximum length l

2.4. Study of the sedimentation efficiency of phytoplankton cell aggregates

Particle sedimentation efficiency was measured using Spillner cylinders with a height of 530 mm and a diameter of 46 mm. The sedimentation efficiency was determined for flocs obtained after the application of an optimal FeCl_3 dose of $20 \text{ mg Fe}^{3+} \cdot \text{L}^{-1}$, an optimal flocculation time of 20 minutes and three velocity gradient ($G=4, 46, 240 \text{ s}^{-1}$). Velocity gradients used in this study were chosen based on the largest differences in the morphological features of the aggregates. After finishing slow mixing, the test materials were transferred from the reaction vessel to Spillner cylinders. The analysis of the impact of aggregates size and shape on the efficiency of sedimentation was made for five arbitrarily selected sedimentation times – 5, 10, 20, 30, 60 min. After each of the assumed sedimentation times, the weight of the sediment was determined by the weight method and the turbidity of the supernatant water by the nephelometric method [22].

3. Results and discussion

3.1 Influence of coagulant dose on aggregate size and size distribution

The effect of coagulant dose on the size of *M. contortum* cell aggregates was determined for the doses of FeCl_3 – 8, 10, 20 and $40 \text{ mg Fe}^{3+} \cdot \text{L}^{-1}$. Coagulant doses were selected based on preliminary studies. Analysis of changes in particle size distributions after the application of FeCl_3 revealed that for all coagulant doses the random variable d_e was a variable with log-normal distribution. After logarithmizing the d_e value, it was found that as a result of using $8 \text{ mg Fe}^{3+} \cdot \text{L}^{-1}$ the aggregates of *M. contortum* formed a monomodal population with an average d_e value of $70.11 \mu\text{m}$ and an σ value of $0.37 (d_e, \mu\text{m})$. The use of higher doses of coagulant (from 10 to $40 \text{ mg Fe}^{3+} \cdot \text{L}^{-1}$) resulted in the transformation of the monomodal distribution into a bimodal distribution, which included discrete particles (Population I) and aggregates of significant equivalent diameter (Population II) (Fig. 1).

The change in the type of particle size distribution resulted from the formation of increasingly larger clusters of cells with an extensive spatial structure and from the increase in their percentage in the entire population of particles. This was confirmed by the values of the parameters μ and σ obtained for the Population II (Table 4). Increasing the d_e value (from $97.51 \mu\text{m}$ at $D_c = 10 \text{ mg Fe}^{3+} \cdot \text{L}^{-1}$ to $126.47 \mu\text{m}$ at $D_c = 40 \text{ mg Fe}^{3+} \cdot \text{L}^{-1}$) indicated that with an increase of coagulant dose, the distribution of the variable shifted consistently towards larger values of the equivalent diameter. At the same time, the increase in value of the standard deviation from $0.18 (d_e, \mu\text{m})$ to $0.26 (d_e, \mu\text{m})$ meant that the range of d_e

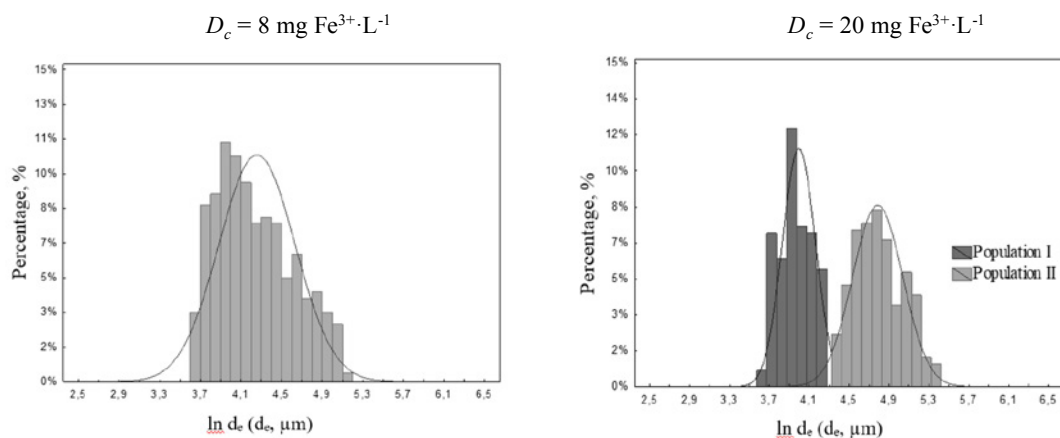


Fig. 1. Distribution of the equivalent diameter (d_e) of *M. contortum* particles after coagulation

Rys. 1. Rozkład średnicy równoważnej (d_e) cząstek *M. contortum* po koagulacji

Table 4. Statistical analysis results of equivalent diameters (d_e) of *M. contortum* cell aggregates after FeCl_3 coagulation
Tabela 4. Wyniki analizy statystycznej średnic równoważnych (d_e) agregatów komórek *M. contortum* po koagulacji FeCl_3

Dc, mg $\text{Fe}^{+3} \cdot \text{L}^{-1}$	No. of particles	Pct., %	Expected value		SD, σ (ln d_e)	Min. (ln d_e)	Max. (ln d_e)	Median (ln d_e)
			d_e , μm	ln d_e				
Log-normal distribution (monomodal)								
8	734	100	70.11	4.25	0.37	3.69	5.11	4.18
Log-normal distribution (bimodal)								
Population I								
10	521	58	54.60	4.00	0.16	3.69	4.30	4.02
20	302	46	54.05	3.99	0.17	3.69	4.30	3.96
40	236	32	52.46	3.96	0.15	3.70	4.30	3.94
Population II								
10	382	42	97.51	4.58	0.18	4.30	4.95	4.56
20	348	54	117.92	4.77	0.25	4.34	5.34	4.73
40	504	68	126.47	4.84	0.26	4.31	5.90	4.82

value was greater. Increasing values of σ indicated a flattening of particle size distributions as a consequence of the appearance of large aggregates.

3.2. Influence of velocity gradient on the flocs properties

3.2.1. Aggregate size

During orthokinetic aggregation, the floc properties depend on the hydrodynamic conditions in the flocculating system, described by a velocity gradient (G). Aggregation of *M. contortum* and *M. aeruginosa* cells at variable rotational speeds of the stirrer, determined the log-normal particle size distribution. In all cases analyzed, the distribution was bimodal. The Fig. 2 shows the dependence of the mean equivalent diameter of aggregates (Population II) on the velocity gradient (G), which was described by a power function. Observations of changes in the size of aggregates, influenced by increasing rotational speed of the mixer, indicated that for both species of phytoplankton the optimal velocity gradient (G) was 4 s^{-1} . After using $G = 4 \text{ s}^{-1}$ the average equivalent diameter of the aggregates reached the highest values of $131.63 \mu\text{m}$ in the case of *M. contortum* and $91.83 \mu\text{m}$ in the case of *M. aeruginosa* (Fig.2).

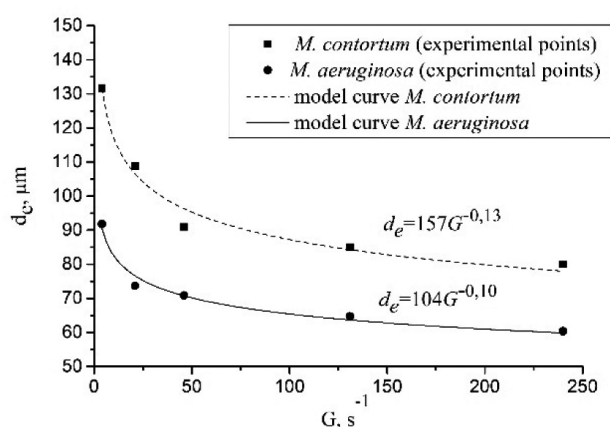


Fig. 2. Changes in the mean equivalent diameter (d_e) of *M. contortum* and *M. aeruginosa* cell aggregates occurring as a result of an increasing velocity gradient (G)

Rys. 2. Zmiany średniej średnicy równoważnej (d_e) agregatów komórek *M. contortum* i *M. aeruginosa* zachodzące pod wpływem wzrastającego gradientu prędkości (G)

In addition, the quantitative analysis of changes in particle size distributions, both for the two species tested, indicated that the dominant share in the total population of particles (58-59%) were the aggregates of the largest size. It was explained that in the case of $G = 4 \text{ s}^{-1}$ there were effective collisions between phytoplankton cells, and the shear forces did not break the aggregates. With the increase in the amount of energy introduced into the flocculating system, the size of aggregates has decreased. For $G = 240 \text{ s}^{-1}$, the average d_e value of the aggregates was $80.64 \mu\text{m}$ and $60.34 \mu\text{m}$ for *M. contortum* and *M. aeruginosa*, respectively. It was found that as the mixing intensity increased, hydrodynamic forces dominated over cohesion forces. It can be assumed that as a result of shear forces, the aggregates disintegrated, according to the surface erosion mechanism [15]. This mechanism led to the disintegration of the aggregate into a large number of particles of a much smaller size, compared to the parent particle, which was observed as an increase in the percentage of discrete particles (Population I). The share of particles with the smallest diameters in the case of *M. contortum* after applying the stirring speed of 10 rpm ($G = 4 \text{ s}^{-1}$) was 42%, while after using the highest rotational speed of the stirrer ($G = 240 \text{ s}^{-1}$) it reached 70%. A similar trend was observed for changes of *M. aeruginosa*. The percentage of discrete particles increased from 41% to 56%. Similar effect was also observed by Chekli et al. [8] during research on coagulation of *Chlorella vulgaris* (*Chlorophyta*) cells using iron chloride (FeCl_3), titanium tetrachloride (TiCl_4) and polytetan tetrachloride (PTC). The d_{50} value (median equivalent diameter) after application of the stirrer rotational speed equal to 40 rpm was $820 \mu\text{m}$, $1195 \mu\text{m}$ and $1310 \mu\text{m}$ for FeCl_3 , TiCl_4 and PTC respectively. Increasing the agitator rotational speed to 200 rpm reduced the size of aggregates by 70% for all coagulants used. The d_{50} value was $270 \mu\text{m}$ (FeCl_3), $325 \mu\text{m}$ (TiCl_4) and $335 \mu\text{m}$ (PTC). Aggregate size reduction due to the increasing velocity gradient was also observed by Bubakova and Pivonsky [3] during research on surface water treatment from the Svihov Reservoir (Czech Republic). Coagulation was carried out using $\text{Fe}_2(\text{SO}_4)_3$. The average equivalent diameter of aggregates formed using the smallest velocity gradient ($G = 28 \text{ s}^{-1}$) was $1330 \mu\text{m}$, while in the case of $G = 307 \text{ s}^{-1}$ it was reduced to $56 \mu\text{m}$. A similar trend was observed when analyzing changes in the maximum equivalent diameter of aggregates, which decreased from $6918 \mu\text{m}$ to $249 \mu\text{m}$. It was found that along with the increase in the G value, aggregate size distributions presented

in the form of a cumulative curve, shifted towards lower values of d_e . The influence of stirring speed on the size of aggregates was also noted by Yu et al. [28] when analyzing the process of coagulation of kaolin suspension using $Al_2(SO_4)_3$. The increase in stirring speed from 40 rpm to 100 rpm reduced the average aggregate size from 250 μm to 40 μm .

3.2.2. Aggregate morphological parameters and fractal structure

For both phytoplankton species, along with the increase in the amount of energy introduced into the system during mixing, a tendency to elongation of cell aggregates was observed. The value of „elongation” of aggregates increased from 0.40 to 0.61 in the case of *M. contortum* and from 0.30 to 0.45 in the case of *M. aeruginosa* (Fig. 3). In addition, increasing the mixing speed resulted in a decrease in the D_1 value (Fig. 4), which indicated an increasingly more regular edge line of the aggregates. Furthermore, the spatial structure of the flocs was less compact (Fig. 3). A relationship between the „solidity” parameter and the second fractal dimension (D_2) was observed. Along with decreasing value of the „solidity” parameter (from 0.63 to 0.40 and from 0.73 to 0.52 for algae and cyanobacteria aggregates, respectively) (Fig. 3) the D_2 value of aggregates was reduced (from 1.72 to 1.20 in the case of *M. contortum* and from 1.93 to 1.70 in the case of *M. aeruginosa*) (Fig. 4). Changes in the spatial structure of the aggregates resulted from the paw mixers used in the tests, producing mainly a circular (peripheral) liquid stream, which allowed particles to move along in the direction of the current line, i.e. around the axis of the mixer causing the aggregates to lengthen and increase their porosity.

During the analysis of the impact of the velocity gradient on the spatial structure of the flocs, morphological differences of aggregates between the studied phytoplankton species were noted. *M. aeruginosa* aggregates were characterized by smaller „elongation” and a more compact structure. These differences were probably due to the shape of individual phytoplankton cells. Circular-shaped *M. aeruginosa* cells formed aggregates with a more regular structure and greater packing of individual cells.

3.3. Time evolution of aggregate size

Changes in the size of aggregates of *M. contortum* and *M. aeruginosa* cells depending on the duration of flocculation, were analyzed on the basis of quantitative and volume distribution curves. The volume distribution of aggregates, described better the changes occurring in the population of the largest aggregates (low sensitivity to small volume flocs). Changes occurring during aggregation in the entire population of particles were observed on the basis of quantitative particle size distributions. Fig. 5a presents volume distribution of aggregates of *M. contortum* cells obtained after flocculation time of 4, 10 and 20 minutes. For both studied species, the particle size distribution curves shifted with increasing flocculation time towards larger values of the equivalent diameter as a consequence of the appearance of larger aggregates. Exceeding the flocculation time of 20 minutes caused a shift in the size distribution of aggregates towards lower d_e values (Fig. 5b), which indicated the breakdown of some aggregates by detaching small fragments or individual cells. Therefore, for the studied phytoplankton species, the optimal flocculation time was 20 minutes.

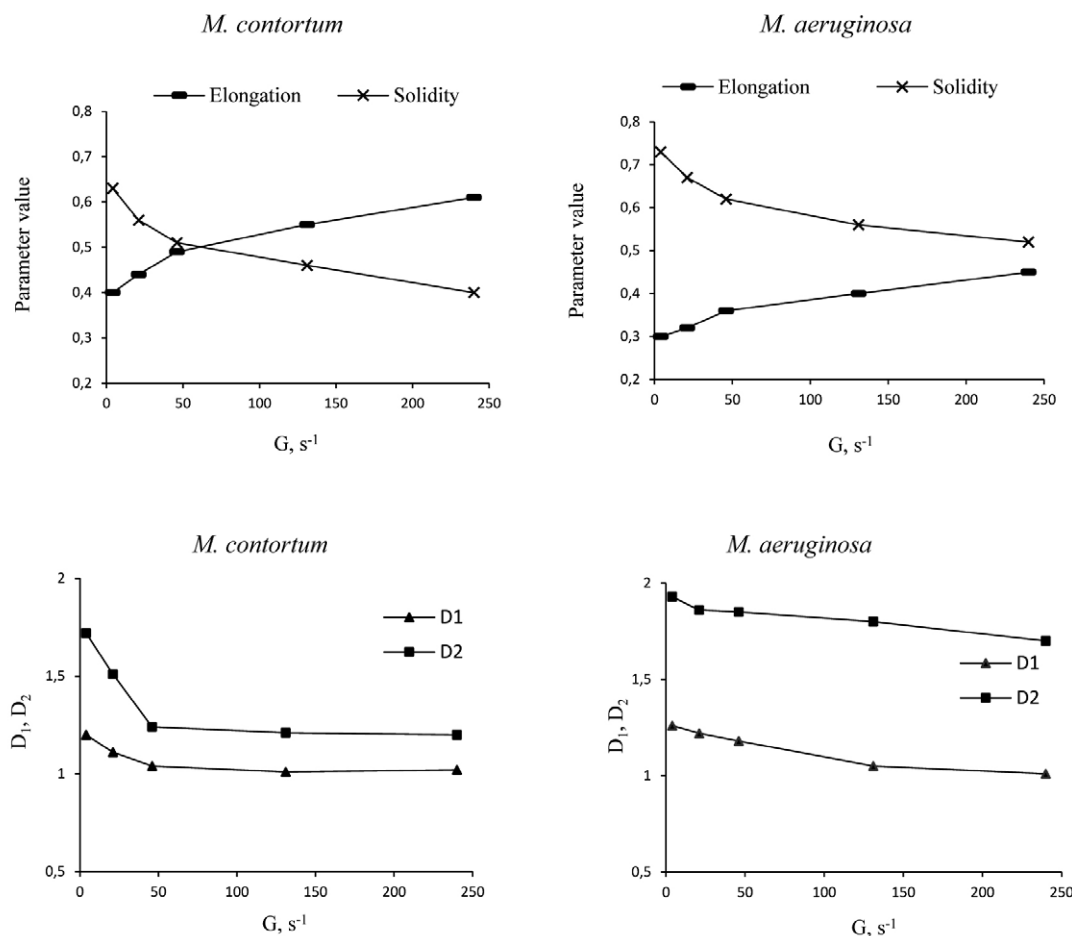
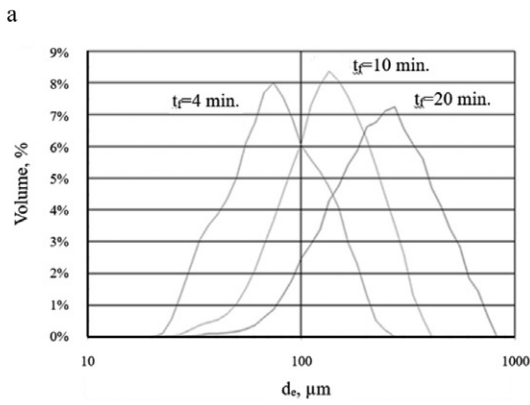


Fig. 3. Changes in the average value of morphological parameters of *M. contortum* and *M. aeruginosa* aggregates under the influence of increasing velocity gradient (G)

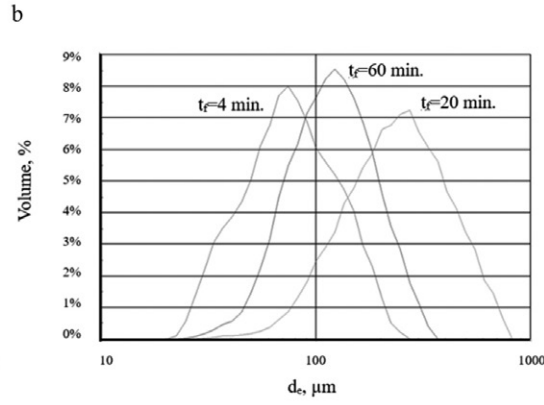
Rys. 3. Zmiany średniej wartości parametrów morfologicznych agregatów *M. contortum* i *M. aeruginosa* pod wpływem wzrastającego gradientu prędkości (G)

Fig. 4. Impact of velocity gradient (G) on fractal dimensions D_1 and D_2 of aggregates of *M. contortum* and *M. aeruginosa* cells

Rys. 4. Wpływ gradientu prędkości (G) na wymiary fraktalne D_1 i D_2 agregatów komórek *M. contortum* i *M. aeruginosa*



M. contortum



M. aeruginosa

Fig. 5. Volume distribution of the equivalent diameter (d_e) of *M. contortum* aggregates for flocculation times $t_f = 4, 10, 20$ min. (a) and $t_f = 4, 20, 60$ min (b)

Rys. 5. Rozkłady objętościowe średnicy równoważnej (d_e) agregatów *M. contortum* dla czasów flokulacji $t_f = 4, 10, 20$ min. (a) i $t_f = 4, 20, 60$ min. (b)

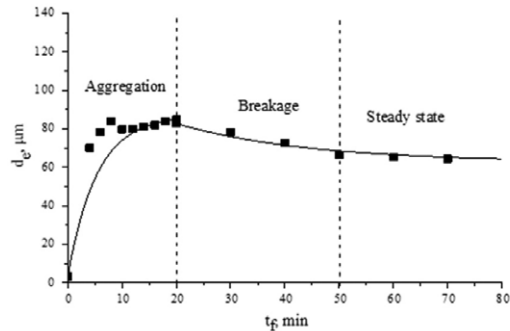
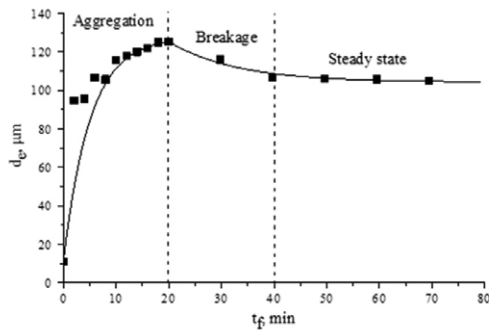


Fig. 6. Changes in mean equivalent diameter (d_p) of population II particles occurring during flocculation of *M. contortum* and *M. aeruginosa* cells

Rys. 6. Zmiany średnicy średnicy równoważnej (d_p) cząstek populacji II zachodzące w czasie flokulacji komórek *M. contortum* i *M. aeruginosa*

Based on the quantitative particle size distributions, it was found that the size of *M. contortum* and *M. aeruginosa* aggregates, after a given flocculation time, described the function with log-normal distribution. Changes in the mean equivalent diameter of *M. contortum* and *M. aeruginosa* cell aggregates (population II) over time are shown in Fig 6.

The research shows that aggregate size evolution, at a constant velocity gradient, occurred in three stages. The multi-stage course of flocculation was also suggested by Francois [12], who distinguished three stages of particle aggregation: the appearance of small flocs of metal hydroxides (I), a rapid increase in aggregates (II) and a decrease in the rate of aggregation of particles until reaching the state of equilibrium, where the aggregate size ceases to increase (III). During the research, no initial phase of aggregation of phytoplankton cells was observed, during which the aggregate size increased exponentially. This was due to the

fact that the analysis of floc size changes was carried out after the rapid mixing was completed. In addition, the test methodology used, did not allow the collection of water samples containing the aggregates formed with such a high frequency. The experimental data obtained during the research allowed to observe the stage corresponding to the lower dynamics of the aggregate size increase, the breakage of formed aggregates and the stage related to steady state. Three evolution phases of aggregate size was observed by Bubakova et al. [4] – aggregate growth (PI), aggregate break-up and/or restructuring (PII) and steady state (PIII).

3.4. Sedimentation properties of phytoplankton aggregates with a fractal structure

The Fig. 7 shows changes in post-coagulation sludge concentration depending on the sedimentation time for the three selected velocity gradients ($G = 4, 46$ and 240 s^{-1}). With the increase

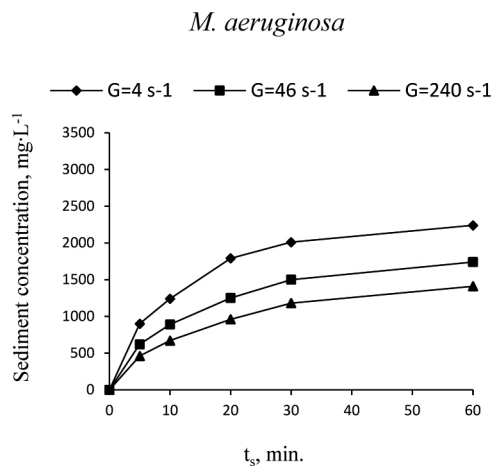
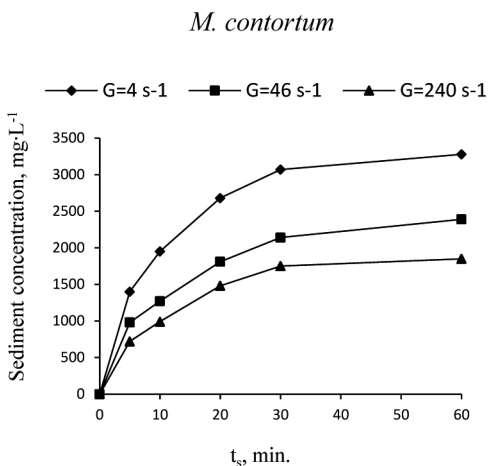


Fig. 7. Changes in sediment concentration based on sedimentation time for the three selected velocity gradients (G)

Rys. 7. Zmiana stężenia osadu od czasu sedymentacji dla trzech wybranych gradientów prędkości (G)

of sedimentation time the concentration of sediment, resulting from the aggregation of phytoplankton cells, increased for all analyzed velocity gradients. The highest sediment concentrations were observed after application $G=4\text{ s}^{-1}$. For example, after a sedimentation time t_s of 5 minutes, the sediment concentration was $1400\text{ mg}\cdot\text{dm}^{-3}$ in the case *M. contortum* and $900\text{ mg}\cdot\text{dm}^{-3}$ in the case *M. aeruginosa*. Increasing the velocity gradient led to a decrease in the removal efficiency of cell aggregate suspension of both phytoplankton species. After application of the stirrer rotational speed of 50, as well as 150 rpm ($G = 46$ and 240 s^{-1}) ($t_s = 5$ minutes) the sediment concentration was lower and amounted respectively to 980 and $720\text{ mg}\cdot\text{L}^{-1}$ (*M. contortum*) and 620 and $460\text{ mg}\cdot\text{L}^{-1}$ (*M. aeruginosa*).

With the increase in the amount of removed suspension over time, the turbidity of water systematically decreased (Fig. 8). The turbidity of the water after sedimentation varied significantly depending on the stirrer rotation speed used during slow mixing. For both phytoplankton species, the best effects of removal of post-coagulant suspension were after applying a stirrer rotation speed of 10 rpm ($G = 4\text{ s}^{-1}$). The turbidity of water reached its lowest value after a sedimentation time of 60 minutes, equal to 5 NTU (*M. contortum*) and 4 NTU (*M. aeruginosa*). Changes in sediment concentration and changes in supernatant water turbidity, depending on sedimentation time for the three selected velocity gradients, determined the impact of aggregate size and structure on sedimentation efficiency. In the case of *M. contortum*, the 20% reduction in sediment concentration (by 16% – *M. aeruginosa*) observed between the smallest and largest velocity gradient after the sedimentation time $t_s = 30$ minutes, resulted from the reduction of the equivalent diameter of aggregates from $131.63\text{ }\mu\text{m}$ to $80.64\text{ }\mu\text{m}$ (from $91.83\text{ }\mu\text{m}$ to $60.34\text{ }\mu\text{m}$ – *M. aeruginosa*) caused by shear forces. Aggregates with a smaller equivalent diameter descended at a lower speed. The decrease in sedimentation efficiency was also affected by decreasing solidity of aggregates with the increase of G value. In the case of *M. contortum*, the „solidity” of aggregates decreased from 0.63 to 0.40 for the smallest and largest velocity gradient G respectively (Fig. 3). In contrast, the „solidity” of *M. aeruginosa* aggregates decreased from 0.73 ($G = 4\text{ s}^{-1}$) to 0.52 ($G = 240\text{ s}^{-1}$) (Fig. 3). It was found that a decrease in the degree of packing of individual cells in the aggregate structure, expressed by a decreasing parameter of „solidity”, probably determined a lower density of aggregates, and thus a lower efficiency of sedimentation.

Comparing the studied phytoplankton species in terms of their removal efficiency, the difference between them was 7% in case of the smallest velocity gradient. For $G = 46$ and 240 s^{-1} , the removal efficiency of both phytoplankton species was at a similar

level. Despite the fact that aggregates of *M. aeruginosa* were characterized by smaller values of d_e ($d_e = 90.92\text{ }\mu\text{m}$ ($G = 46\text{ s}^{-1}$), $d_e = 80.64\text{ }\mu\text{m}$ ($G = 240\text{ s}^{-1}$) – *M. contortum*; $d_e = 70.81\text{ }\mu\text{m}$ ($G = 46\text{ s}^{-1}$), $d_e = 60.34\text{ }\mu\text{m}$ ($G = 240\text{ s}^{-1}$) – *M. aeruginosa*), they descended at a speed similar to the speed of *M. contortum* aggregates. It was found that the morphological features of the flocs had an impact on the aggregate sedimentation efficiency. *M. aeruginosa* aggregates were characterized by greater „solidity” („solidity” = 0.51 ($G = 46\text{ s}^{-1}$), „solidity” = 0.40 ($G = 240\text{ s}^{-1}$) – *M. contortum*; „solidity” = 0.62 ($G = 46\text{ s}^{-1}$), „solidity” = 0.52 ($G = 240\text{ s}^{-1}$) – *M. aeruginosa*), and thus probably higher density, which decided to increase their sedimentation speed. The impact of spatial structure of aggregates on sedimentation efficiency was also observed during research conducted by Aouabed et al. [1]. Post-coagulation aggregates, despite their considerable size ($860\text{--}890\text{ }\mu\text{m}$), fell at a low speed of $0.7\text{ mm}\cdot\text{s}^{-1}$. According to the authors, the results obtained were due to the irregular spatial structure and significant porosity of the aggregates (*Shape Factor SF* = 0.12-0.15; $D_2 = 1.51\text{--}1.55$; $D_2 = 1.91\text{--}1.99$), and thus low mass-volume concentration of particles ($3\text{ kg}\cdot\text{m}^{-3}$). The sedimentation speed did not increase depending on the the particle diameter square powered, as assumed by the Stokes formula. The aggregate descending speed depended on the spatial structure of the aggregates, which changed along with the conditions of the coagulation and flocculation process. According to Vahedi and Gorczyca [27], the sedimentation speed is determined by the density (mass distribution) of post-coagulation aggregates, depending on the aggregation mechanism, the type of primary particles and the degree of their packing in the aggregate structure. Chakroborti et al. [6] also observed differences in the efficiency of post-coagulation aggregate removal in the sedimentation process depending on the coagulation mechanism and spatial structure of aggregates.

In conclusion, determining the optimal conditions for coagulation and flocculation of phytoplankton, ensuring the largest possible effective number of collisions between cells while maintaining the delicate structure of flocs, requires careful analysis of changes in the size and shape of the formed aggregates. The measuring method used in the work and the phytoplankton organisms used in the study allowed the assessment of the possibility of obtaining aggregates characterized by different sizes and spatial structure, depending on the conditions of the coagulation and flocculation process. Changes in the size of aggregates were visible as changes in quantitative and volume distributions as well as changes in the percentage of discrete particles and aggregates of significant size. Based on the conducted research, it was found that in order to obtain aggregates of the largest possible sizes, the process of coagulation and flocculation of *M. contortum* and

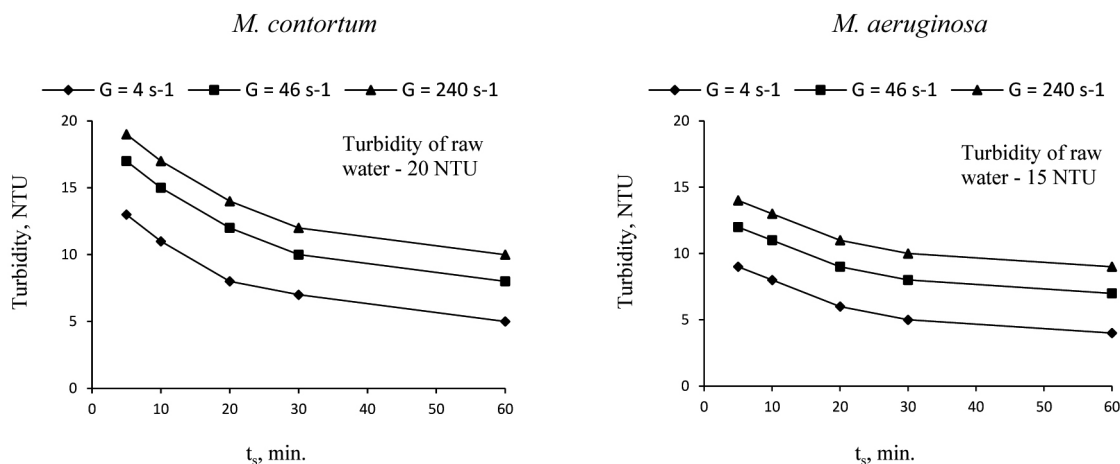


Fig. 8. Changing the turbidity based on sedimentation time for the three selected velocity gradients

Rys. 8. Zmiana mętności wody od czasu sedymentacji dla trzech wybranych gradientów prędkości

M. aeruginosa cells, with a concentration of 8.6×10^7 and 9.0×10^7 cells·L⁻¹, respectively, should be carried out with the following conditions: $D_c = 20$ mg Fe³⁺·L⁻¹, $G = 4$ s⁻¹ and $t_f = 20$ minutes. Due to the highly irregular and complicated shape of aggregates, they were considered to be fractal objects. The morphological diversity of aggregates observed in changes in fractal dimensions was confirmed by the values of the determined morphological parameters. Based on the conducted research, it could be stated that the differences in the shape of aggregates also resulted from the different spatial structure of individual phytoplankton cells. The size and spatial structure of aggregates influenced the sedimentation properties of aggregates.

4. Conclusions

1. The microscopic image analysis used in the research and the use of the principles of fractal geometry allowed the selection of aggregation conditions for *M. contortum* and *M. aeruginosa* cells, enabling the effective removal of these phytoplankton representatives from the water in the sedimentation process.
2. Size of phytoplankton cell aggregates was subordinated to log-normal distribution. The analysis of changes in aggregate size distribution indicated that along with the increase of coagulant doses (D_c) and flocculation time (t_f), their mean equivalent diameter increased. The average diameter of aggregates, on the other hand, decreased with increasing velocity gradient (G).
3. Along with the increase in the amount of energy introduced into the system during mixing (G), a tendency to elongate cell aggregates and reduce their solidity was observed. The morphological characteristics of phytoplankton aggregates based on morphological parameters and fractal geometry allowed to observe a significant relationship between D_2 and „solidity”. An increase in the morphological parameter in the form of „solidity” was associated with an increase in the value of the second fractal dimension.
4. Aggregate size evolution, at a constant velocity gradient, occurred in three stages: aggregate growth (I), aggregate break-up (II) and steady state (III).
5. The effectiveness of the sedimentation process was determined by the size and solidity of the aggregates. The reduction of the mean equivalent diameter and „solidity” of aggregates resulted in a slower sedimentation rate of aggregates. ■

REFERENCES

- [1] Aouabed Ali, Djamal Eddine Hadj-Boussaad, Roger Ben-Aim. 2008. „Morphological characteristics and fractal approach of the flocs obtained from natural organic matter extract of water of the Keddara dam (Algeria)”. *Desalination* 231 (1-3) : 314-322.
- [2] Bąk Małgorzata, Andrzej Witkowski, Joanna Żelazna-Wieczorek, Agata Wojtal, Ewelina Szczepocka, Katarzyna Szulc, Bogusław Szulc. 2012. *Klucz do oznaczania okrzemek w fitobentosie na potrzeby oceny stanu ekologicznego wód powierzchniowych w Polsce*. Warszawa: Biblioteka Monitoringu Środowiska.
- [3] Bubakova Petra, Martin Pivovsky. 2012. „The influence of velocity gradient on properties and filterability of suspension formed during water treatment”. *Separation and Purification Technology* 92 : 161-167.
- [4] Bubakova Petra, Martin Pivovsky, Filip Petr. 2013. „Effect of shear rate on aggregate size and structure in the process of aggregation and at steady state”. *Powder Technology* 235 : 540-549.
- [5] Cannell Richard. 1993. „Algae as a source of biologically active products”. *Pest Management Science* 39 (2) : 147-153.
- [6] Chakraborti Rajat K., Joseph Atkinson, John Van Benschoten. 2000. „Characterization of alum floc by image analysis”. *Environmental Science and Technology* 34 (18) : 3969-3976.
- [7] Chakraborti Rajat K., Kevin H. Gardner, Joseph F. Atkinson, John E. Van Benschoten. 2003. „Changes in fractal dimension during aggregation”. *Water Research* 37 (4) : 873-883.
- [8] Chekli Laura, C. Eripret, Sunghyuk Park, S. Tabatabai, O. Vronska, Bojan Tamburic, Jongho Kim, Hokyong Shon. 2017. „Coagulation performance and floc characteristics of polytitanium tetrachloride (PTC) with titanium tetrachloride (TiCl₄) and ferric chloride (FeCl₃) in algal turbid water”. *Separation and Purification Technology* 175 : 99-106.
- [9] Chow Christopher W. K., Mary Drikas, Jenny House, Michael D. Burch, Renate M.A. Velzeboer. 1999. „The impact of conventional water treatment processes on cells of the cyanobacterium *Microcystis aeruginosa*”. *Water Research* 33 (15) : 3253-3262.
- [10] Demir Nilsun, Serap Pulatsu, Mine Kirkagac, Akasya Topcu, Ozge Zencir Tanir, Ozden Fakioglu. 2011. „Phytoplankton composition considering the odor occurrence in Porsuk River (Eskisehir-Turkey)”. *Asian Journal of Chemistry* 23 (1) : 247-250.
- [11] Falconer Ian R., Andrew R. Humpage. 2005. „Health risk assessment of Cyanobacterial (blue-green algal) toxins in drinking water”. *International Journal of Environmental Research and Public Health* 2 (1) : 43-50.
- [12] Francois R. J. 1988. „Growth kinetics of hydroxide flocs”. *Journal American Water Works Association* 80 (6) : 92-96.
- [13] Gonzalez-Torres Andrea, J. Putnam, Bruce Jefferson, Richard M. Stuetz, Rita K. Henderson. 2014. „Examination of the physical properties of *Microcystis aeruginosa* flocs produced on coagulation with metal salts”. *Water Research* 60 : 197-209.
- [14] ISO 9276-6: 2008. „Representation of results of particle size analysis. Part 6: Descriptive and quantitative representation of particle shape and morphology”.
- [15] Jarvis Peter, Bruce Jefferson, John Gregory, Simon Parsons. 2005. „A review of floc strength and breakage”. *Water Research* 39 (14) : 3121-3137.
- [16] Jiang Qing, Bruce E. Logan. 1996. „Fractal dimensions of aggregates from shear devices”. *Journal American Water Works Association* 88 (2) : 100-113.
- [17] Jodłowski Andrzej, Ewelina Gutkowska. 2015. „Wpływ warunków flokulacji na cechy morfologiczne i wymiary fraktalne agregatów komórek glonów”. *Instal* 12 : 79-82.
- [18] Kotai J. 1972. „Instructions for the Preparation of Modified Nutrient Solution Z8 for Algae”. *Norwegian Institute for Water Research Publication B-11/(69)* : 5.
- [19] Oliveira Cristiane, Rafael Teixeira Rodrigues, Jorge Rubio. 2010. „A new technique for characterizing aerated flocs in a flocculation-microbubble flotation system”. *International Journal of Mineral Processing* 96 (1-4) : 36-44.
- [20] Perez Y. G., Selma Leite, Maria Alice Coelho. 2006. „Activated sludge morphology characterization through an image analysis procedure”. *Brazilian Journal of Chemical Engineering* 23 (3) : 319-330.
- [21] Picińska-Fałtynowicz Joanna, Jan Błachuta. 2012. *Klucz do identyfikacji organizmów fitoplanktonowych z rzek i jezior dla celów badań monitoringowych części wód powierzchniowych w Polsce*. Warszawa: Biblioteka Monitoringu Środowiska.
- [22] PN-EN ISO 7027-1:2016-09. „Water quality. Determination of turbidity”.
- [23] Rekar S., Frantisek Hindák. 2002. „Aphanizomenon slovenicum sp. nov.: morphological and ecological characters of a new cyanophyte/cyanobacterial species from Lake Bled, Slovenia”. *Annales de Limnologie – International Journal of Limnology* 38(4) : 271-285.
- [24] Runnegar Maria, Norbert Berndt, Neil Kaplowitz. 1995. „Microcystin uptake and inhibition of protein phosphatases: effects of chemoprotectants and self-inhibition in relation to known hepatic transporters”. *Toxicology and Applied Pharmacology* 134 (2) : 264-272.
- [25] Sillanpaa Mika, Mohamed Chaker Ncibi, Anu Matilainen, Mikko Vepsäläinen. 2018. „Removal of natural organic matter in drinking water treatment by coagulation: A comprehensive review”. *Chemosphere* 190 : 54-71.
- [26] Uher Bohuslav. 2007. „Morphological characterization of three subaerial *Ca*-loithrix species (Nostocales, Cyanobacteria)”. *Fottea* 7(1) : 33-38.
- [27] Vahedi Arman, Beata Gorczyca. 2014. „Settling velocities of multifractal flocs formed in chemical coagulation process”. *Water Research* 53 : 322-328.
- [28] Yu Wen-zheng, John Gregory, Luiza Campos, Guibai Li. 2011. „The role of mixing conditions on floc growth, breakage and re-growth”. *Chemical Engineering Journal* 171 (2) : 425-430.